

Supporting Information

Covalent organic framework membrane with enhanced directional ion nanochannels for efficient hydroxide conduction

Jia Chen^a, Ping Li^a, Ningxin Zhang^a, Shaokun Tang^{a,b,*}

^a Key Laboratory for Green Chemical Technology of Ministry of Education, School of Chemical Engineering & Technology, Tianjin University, Tianjin 300350, China

^b Collaborative Innovation Center of Chemical Science and Engineering (Tianjin), Tianjin University, Tianjin 300350, China

* Corresponding author. Email: shktang@tju.edu.cn

EXPERIMENTAL

1. Materials

1,3,5-triformylbenzene (96%, BeiJing Hua Wei Rui Ke Chemicals Co., Ltd), 2, 5-dihydroxyterephthalic acid diethyl ester (99%, Aladdin, China), 1,4-dioxane (AR, 99%, Aladdin, China), mesitylene (AR, 97%, Aladdin, China), acetic acid (99.5%, Tianjin Jiang Tian Chemical Co., Ltd), N,N-dimethylformamide (DMF, AR, Tianjin concord technology Co., Ltd), tetrahydrofuran (THF, C₄H₈O, Tianjin Yuan Li Chemical Co., Ltd), acetone (AR, 98%, Aladdin, China), dichloromethane (AR, 98%, Aladdin, China), hydrazine hydrate (30 wt%, Aladdin, China), potassium carbonate (K₂CO₃) and potassium iodide (KI) were obtained from Sigma-Aldrich. All reagents were commercially available and used without further purification.

2. Synthesis of COF building units

(1) Synthesis of 2-hydroxy-5-(6-bromopentoxy)-diethyl terephthalate (Q1)

1.05 g 2, 5-dihydroxyterephthalic acid diethyl ester was weighed and dissolved in 30 mL mixed solution (DMF/ acetone =1:2). After stirring for 20 min, 4.12 g potassium carbonate and 200 mg potassium iodide were added. Then, 1.71 g 1, 6-dibromohexane was added to the mixture and stirred at 80 °C for 18 h. After the reaction, the mixture was hot filtered and the filtrate was evaporated to dry. The product was dissolved in deionized water and extracted three times with dichloromethane. The product was purified by column chromatography and dried at 60 °C to obtain 2-hydroxy-5-(6-bromopentoxy)-diethyl terephthalate (Q1).

¹H NMR (500 MHz, CDCl₃): δ = 10.39 (s, 1H), 7.36 (s, 1H), 7.32 (s, 1H), 4.45 (q,

J = 7.1 Hz, 2H), 4.38 (q, J = 7.1 Hz, 2H), 4.00 (t, J = 6.3 Hz, 2H), 3.44 (t, J = 6.8 Hz, 2H), 1.91 (p, J = 6.9 Hz, 2H), 1.84 (p, J = 6.6 Hz, 2H), 1.61-1.48 (m, 4H), 1.45 (t, J = 7.1 Hz, 3H), 1.39 (t, J = 7.1 Hz, 3H).

^{13}C NMR (100 MHz, CDCl_3): δ = 165.18, 164.98, 150.31, 146.15, 129.04, 127.74, 116.32, 114.92, 69.12, 62.65, 61.13, 34.33, 32.63, 29.29, 24.67, 14.31, 14.28.

(2) Synthesis of 2-hydroxy-5-(trimethylammonium-pentoxo)-diethyl terephthalate (Q2)

1.05 g Q1 was dissolved in 20 mL ethanol solution (EtOH) and 5 mL trimethylamine solution (30 wt%) was added. After stirred at room temperature for 48 h and dried in vacuum at 60 °C for 24 h, white solid of 2-hydroxy-5-(trimethylammonium pentoxo)-diethyl terephthalate (Q2) was obtained.

^1H NMR (500 MHz, CDCl_3): δ = 10.12 (s, 1H), 7.33 (s, 1H), 7.18 (s, 1H), 4.36 (q, J = 7.1 Hz, 2H), 4.27 (q, J = 7.1 Hz, 2H), 3.97 (t, J = 6.2 Hz, 2H), 3.31-3.24 (m, 2H), 3.05 (s, 10H), 1.72 (dd, J = 14.0, 7.0 Hz, 2H), 1.70-1.64 (m, 2H), 1.48 (p, J = 7.6 Hz, 2H), 1.31 (dt, J = 21.4, 7.1 Hz, 8H).

^{13}C NMR (100 MHz, CDCl_3): δ = 168.93, 166.38, 153.14, 150.00, 126.49, 119.29, 115.46, 113.74, 69.38, 66.67, 62.70, 62.42, 52.94, 28.48, 25.58, 25.17, 22.50, 13.72, 13.56.

(3) Synthesis of 2-hydroxy-5-(trimethylammonium-pentoxo)-p-phenylhydrazide (Q3)

1.05 g Q2 was dissolved in 30 mL ethanol solution, and added 3 mL hydrazine

hydrate (30 wt%). After stirred at 80 °C for 12 h and dried at 60 °C under vacuum for 24 h, 2-hydroxy-5-(trimethylammonium pentoxy)-p-phenylhydrazide (Q3) was obtained. The synthesis process of building units is shown in Fig. S1.

^1H NMR (500 MHz, CDCl_3): δ = 9.21 (s, 1H), 7.53 (s, 1H), 7.14 (s, 1H), 4.57 (s, 2H), 4.04 (t, J = 6.3 Hz, 2H), 3.36-3.26 (m, 2H), 3.06 (s, 10H), 1.74 (dp, J = 22.8, 7.9, 7.0 Hz, 4H), 1.48 (p, J = 7.5 Hz, 2H), 1.35 (p, J = 6.9 Hz, 2H).

^{13}C NMR (100 MHz, CDCl_3): δ = 166.23, 165.33, 150.03, 149.11, 123.11, 118.60, 118.26, 112.35, 69.61, 66.74, 52.99, 28.25, 25.53, 25.12, 22.45.

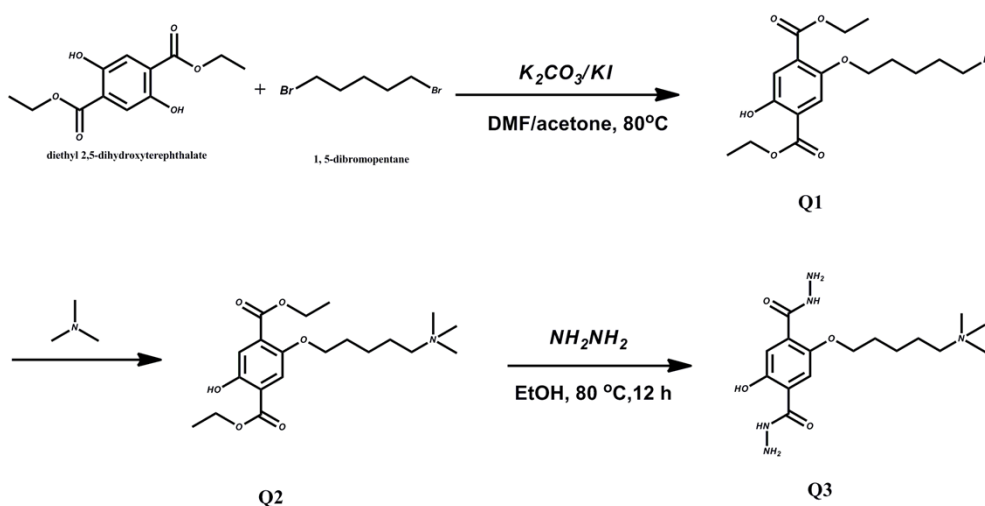


Fig. S1. Synthesis of COF building units

3. Characterizations

Field emission scanning electron microscope (SEM) (HITACHI S-4800) was utilized to observe the morphology.

Transmission electron microscopy (TEM) observation was carried out on an electron microscope (JEM-2100, Japan) with an accelerating voltage of 200 kV.

Powder X-ray diffraction (XRD) patterns were collected on a XRD patterns were

carried out on Bruker using Ni-filtered Cu K α radiation ($\lambda= 0.1541$ nm).

The dispersion of elements was probed by EDX-mapping using the Energy Dispersive X-ray Detector equipping in the TEM.

Fourier transform infrared (FT-IR) spectroscopy was performed by a Bruker VERTEX 70 with the range of wavelength from 4000 to 400 cm^{-1} .

Thermogravimetric analysis (TGA) (NETZSCH-TG209 F3) was utilized to measure the thermal properties of samples at a heating rate of 10 $^{\circ}\text{C}/\text{min}$ under air flow.

The ^1H NMR analysis was recorded on a Bruker spectrometer (500 MHz), using $\text{CDCl}_3\text{-d}_6$ as the solvent, all chemical shifts were referenced relative to tetramethylsilane. ^{13}C NMR analysis was recorded on a Bruker spectrometer (100MHz), using $\text{CDCl}_3\text{-d}_6$ as the solvent.

4. Measurements

The ion exchange capacity (IEC) of samples were determined by a back-titration method [1, 2]. Before titration, samples were dried at 60 $^{\circ}\text{C}$ overnight, then soaked into HCl solution at room temperature for 24 h. With phenolphthalein as the indicator, the residual solution was titrated using standard NaOH aqueous solution. The IEC values (mmol g^{-1}) can be calculated as the following formula:

$$\text{IEC} = \frac{c_{\text{HCl}}V_{\text{HCl}} - c_{\text{NaOH}}V_{\text{NaOH}}}{m} \quad (\text{S1})$$

Where, m represents the weight of samples, c_{HCl} , V_{HCl} , c_{NaOH} and V_{NaOH} represent the concentration and volume of HCl and NaOH, respectively.

Membrane impedance was acquired using an electrochemical workstation

(CompactStat, IVIUM Tech.) by two-probe AC impedance method in a frequency range from 100 kHz to 10 Hz. Before testing, samples were immersed in NaOH solution (1.0 mol L⁻¹) for 24 h, then soaked and washed with deionized water several times. The impedance of the membrane was tested at different temperatures in 100% RH. According to the Nyquist plot, the hydroxide conductivity of the membrane could be calculated via the following relationship:

$$\sigma = \frac{l}{AR} \quad (\text{S2})$$

Where σ (S cm⁻¹) represents the ion conductivity of membranes; l (cm) the distance between two electrodes; A (cm²) the cross-section area of the membrane and R (Ω) the membrane impedance derived from the high frequency intercept with the Re(z)-axis on Nyquist plot.

TJU-1 was dispersed in deionized water, DMF and 2 mol/L NaOH solution respectively. The dispersion of TJU-1 in the solution was observed after 30 days.

The weight (W_{dry}) and length (L_{dry}) of the rectangular dry membrane were measured. Afterwards, the membranes were hydrated in water, and the weight (W_{wet}) and length (L_{wet}) of hydrated membrane were tested. The water uptake and swelling ratio were calculated with the following equations:

$$\text{water uptake (\%)} = \frac{W_{\text{wet}} - W_{\text{dry}}}{W_{\text{dry}}} \times 100 \quad (\text{S3})$$

$$\text{swelling ratio (\%)} = \frac{L_{\text{wet}} - L_{\text{dry}}}{L_{\text{dry}}} \times 100 \quad (\text{S4})$$

The mechanical strengths of the membranes were tested by an electronic

stretching machine (Yangzhou Zhongke WDW-02) at the strain rate of 10 mm min⁻¹.

The Pt/C purchased from Johnson Matthey was mixed with isopropanol solvent to prepare the ink. The loading amount of Pt is 0.5 mg cm⁻² with the electrode area of 1 cm². The membrane-electrode assembly (MEA) consisting of anode/cathode catalyst layers and a TJU-1 COF membrane. The MEA was tested in a fuel cell device at 60 °C with fully humidified H₂ (100 mL min⁻¹) and O₂ (100 mL min⁻¹).

5. Molecular dynamics simulations

The crystal structure of TJU-1 was simulated by Material Studio software, and the standard symmetric stacking structure was obtained. The crystal structure of COF was optimized by using the Forcite and DFTB module with universal force field, the P6 space group was obtained by Pawley refining the crystal cell parameters. The crystal cell parameters were: a=b=30.779 Å, c=4.331 Å; $\alpha=\beta=90^\circ$, $\gamma=120^\circ$. After optimized processing, the simulated XRD of TJU-1 was obtained, which has four characteristic peaks, namely, the lattice spacing of 3.26 Å, 6.89 Å, 8.98 Å and 21.73 Å, respectively. The corresponding crystal faces (100), (200), (210) and (001) are symmetric stacked crystal structures. The simulated periodic crystal structure of the symmetric stacked TJU-1 is shown in Fig. S2, and its cell parameters and atomic coordinates are shown in Table S2.

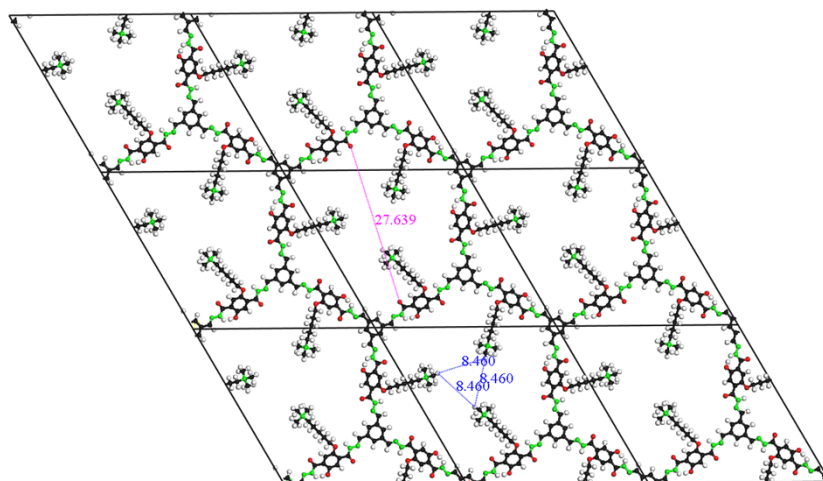


Fig. S2 Simulated unit cells for symmetric stacking modes of TJU-1 (nitrogen is shown in green, oxygen in red, carbon in black, and hydrogen in white).

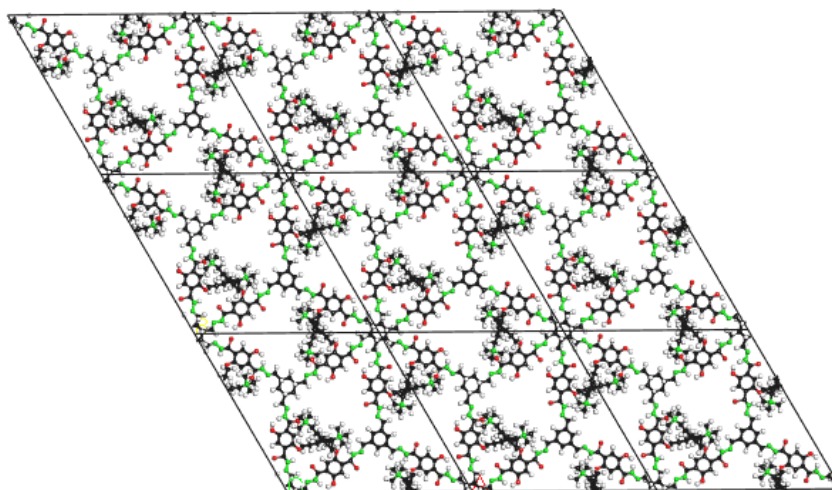


Fig. S3 Simulated unit cells for staggered stacking modes of TJU-1 (nitrogen is shown in green, oxygen in red, carbon in black, and hydrogen in white).

Meanwhile, the DFTB model with universal force field was used to calculate the electrostatic interaction and interlayer interaction energy of COF nanosheets. Firstly, the COF structure was optimized, and then the energy was calculated by DFTB method. The interlayer interaction energy of COF nanosheets were calculated by the

energy difference between two monolithic layers and two laminated layers in the periodic structure. A vacuum layer should be added to ensure the independence of a single sheet in energy calculation.

The periodic structure of a section of TJU-1 was intercepted to build the system model in the Amorphous cell. According to the amounts of QA groups in TJU-1, corresponding amounts of hydroxide ions and water molecules were added, and each OH^- corresponds to 4 H_2O molecules to achieve complete hydration. The kinetic process of OH^- transfer in anion exchange membrane at 100% humidity was simulated. The molecular dynamics (MD) simulation was carried out using the COMPASS force field [3-5], and some modifications were made in the COMPASS force field to adapt to the dynamics simulation of the system. Velocity Verlet algorithm is used to integrate the equation of motion, and the time step is 1.0 fs. The damping relaxation time of the nose-Hoover thermostat used in the NVT and NVE MD simulations was 0.1 ps and the dimensionless cellular factor was 1.0. Amorphous periodic Amorphous cells were constructed by using 3-D Amorphous Cell module of MS. TJU-1 sheets, OH^- and H_2O molecules were added into the Amorphous cells (square boxes).

The initial amorphous structure was constructed at a lower density of 1.00 g cm^{-3} in the MD simulations. Afterwards, the system was relaxed by the annealing procedure in NVT procedure, the initial volume expanded while the temperature increased, and then hold for a period of time, finally the density of system was back to 1.00 g cm^{-3} and the temperature back to the initial level. Such progress was repeated

three times, guaranteeing the system is in equilibrium. When the anneal procedures are completed, NVE simulations were performed to equilibrate the system again. And then the dynamic simulations were continued in equilibrium. 1000 ps NVT simulation was performed for the analyses of the structural and diffusion properties of hydroxide ions and water molecules. In the above simulations, the time step was 0.1 fs. The microphase structure of the optimized system is shown in Fig. S3.

In order to study the structure-activity relationship between the microphase structure of TJU-1 membrane and the diffusion properties of hydroxide ions, the correlation between the quaternary ammonium functional groups and hydroxide ions and water molecules and the diffusion coefficients of hydroxide ions and water molecules in TJU-1 pores were calculated. The radial distribution function (RDF) and the corresponding coordination number (CN) of the oxygen atoms and the nitrogen atoms in the quaternary ammonium group and the oxygen atoms in the hydroxide ions and the water molecules were calculated to reflect the correlation between the oxygen ions and the water molecules and the quaternary ammonium group.

The radial distribution function (RDF) and its corresponding coordination number (CN) were calculated with the following equations [6-9]:

$$RDF(r) = g(r) = \frac{n(r)}{\rho 4\pi r^2 \Delta r} \quad (S5)$$

$$CN = \int_0^r \rho 4\pi r^2 g(r) dr \quad (S6)$$

Where $g(r)$ and CN are RDF and coordination numbers, respectively. $n(r)$ is the number of atoms within the distance r from the central atom, ρ denotes the overall

number density. RDF and CN are obtained by averaging trajectories.

The diffusion constants of ions were determined based on the mean-square displacement (MSD):

$$MSD(m) = \langle |r(t) - r|^2 \rangle = \frac{1}{n} \sum_{i=1}^n |r(m+i) - r(i)|^2 \quad (S7)$$

where r represents the position of the particle in the unfolded trajectory, t is the time, m is denoted the maximum number of points allowed for the MSD calculation, n is the number of data points used for averaging, $m+n$ stands for the total number of frames, and i is the step counter.

In order to ensure the validity of the calculated results, the trajectories of 30 hydroxide ions and water molecules were averaged.

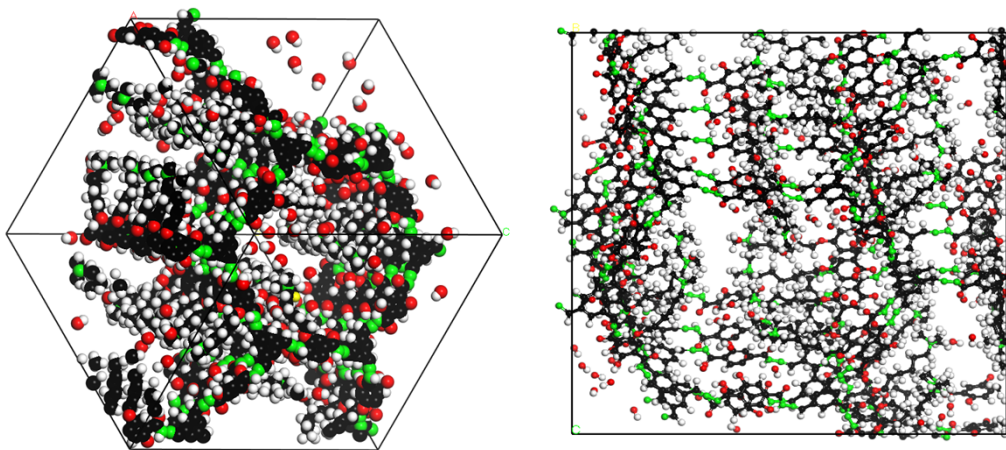


Fig. S4 Nanophase structures of simulated TJU-1 system (nitrogen is shown in green, oxygen in red, carbon in black, and hydrogen in white).

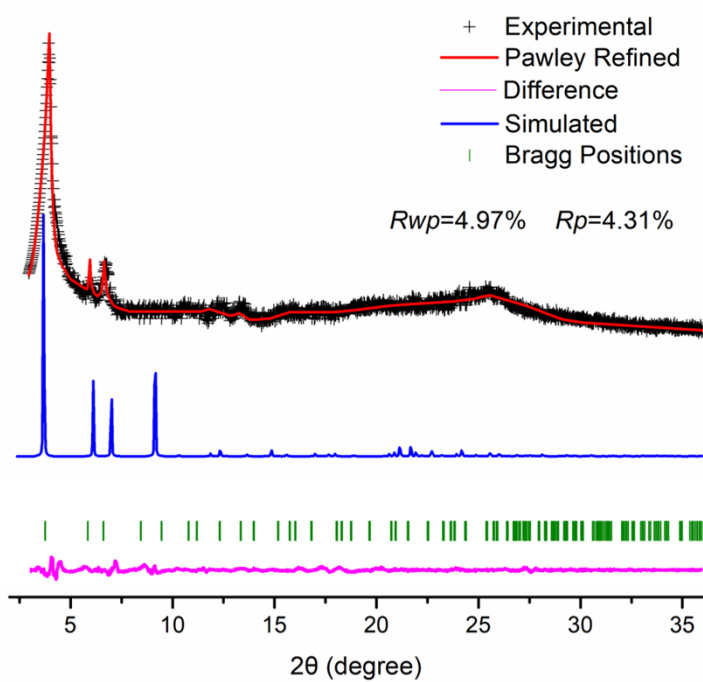


Fig. S5 PXRd patterns of symmetric stacked TJU-1: experimental pattern (black dots), Pawley-refined pattern (red curve), simulated PXRd pattern for eclipsed structure (blue curve), difference plot between the observed and refined PXRd patterns (purple curve).

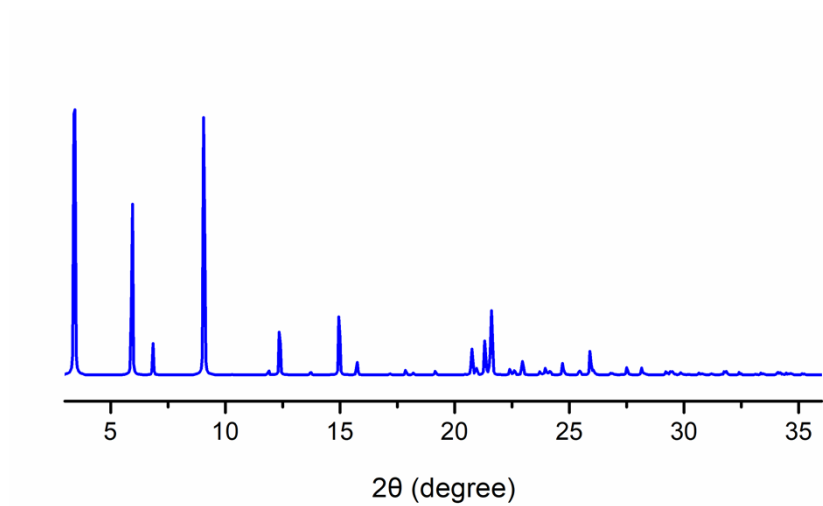


Fig. S6 Simulated PXRD pattern for staggered structure.

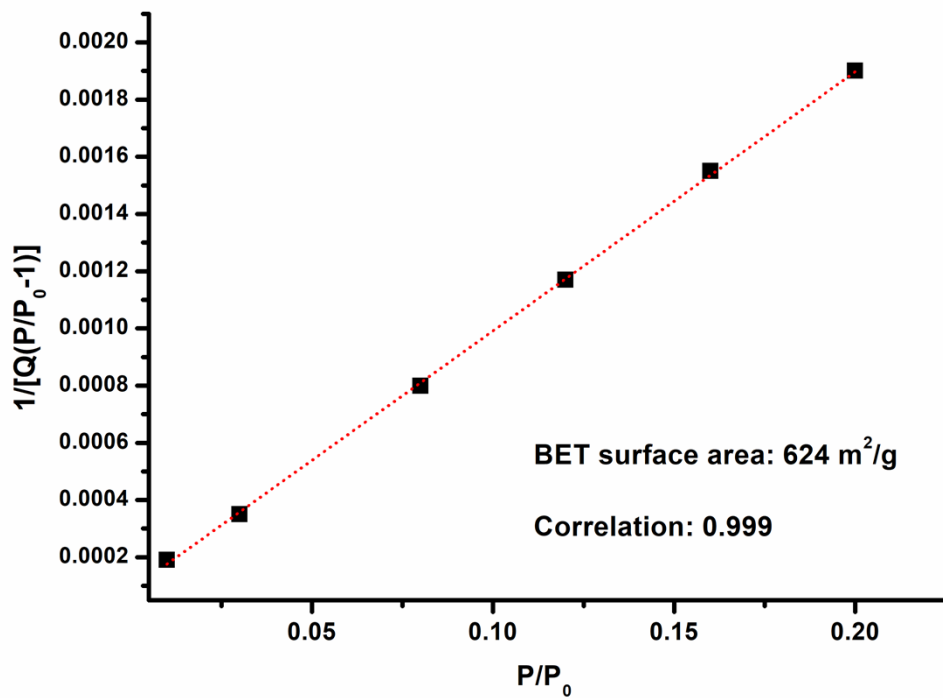


Fig.S7 BET plot of TJU-1 calculated from N₂ adsorption isotherm at 77 K.

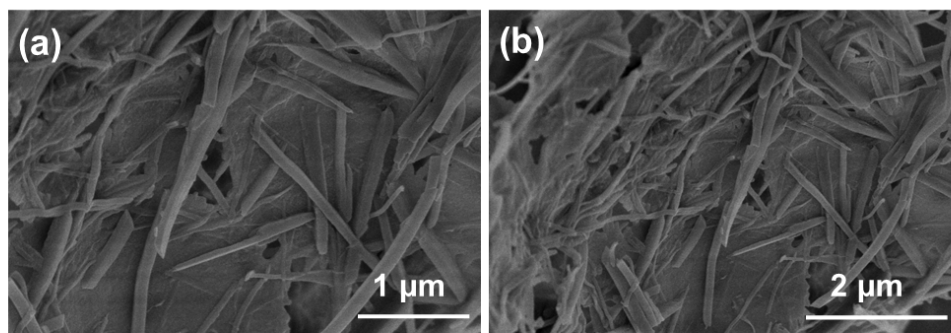


Fig. S8. SEM images of COF TJU-1.

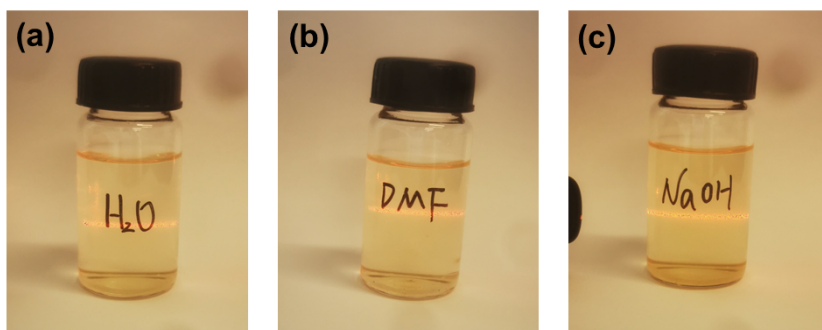


Fig. S9. Photos of TJU-1 powder in various solvents after 30 days: (a) Deionized water (H_2O), (b) N, N-Dimethylformamide (DMF), and (c) 2mol/L NaOH solution.

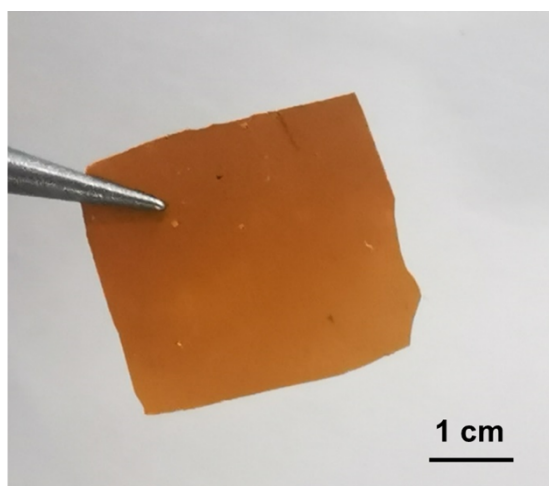


Fig. S10. Photograph of TJU-1 membrane.

Table S1 Comparison of H₂/O₂ single fuel cell performance of the COF-based membranes in this work and other reported typical AEMs

Membrane	Peak power density (mW/cm ²)	Reference
TJU-1	203	This work
QA-PEEK/QA-P(ES1-co-ES2)-20	137	[10]
PPO-TPIIm-30	137	[11]
PTDIB (QPPO)	168.9	[12]
QPPO/PSF/2.0%TiO ₂	118	[13]
QPPEEK-PEG-20	154	[14]
PPO-C-1QA	141	[15]

Table S2 Cell parameters and atomic coordinates of TJU-1

TJU-1: Space group symmetry P3

a = b = 30.779 Å, c = 4.331 Å, $\alpha = \beta = 90^\circ$, $\gamma = 120^\circ$

C1	C	0.94662	0.98559	0.55162
C2	C	0.87034	0.71970	0.36907
C3	C	0.82563	0.70156	0.19536
C4	C	0.79036	0.65033	0.19777
C5	C	0.79905	0.61578	0.35821
C6	C	0.84385	0.63312	0.52839
C7	C	0.87877	0.68522	0.53378
O8	O	0.85065	0.59740	0.69416
C9	C	0.89516	0.61227	0.87117
C10	C	0.94006	0.62242	0.66763
C11	C	0.98477	0.63162	0.86944
O12	O	0.81543	0.73234	0.00765
C13	C	0.75966	0.56178	0.35107
N14	N	0.77159	0.52464	0.32208
O15	O	0.71567	0.55058	0.36588
N16	N	0.73376	0.47383	0.32265
C17	C	0.74414	0.43787	0.30430
C18	C	0.70410	0.38447	0.30521
C19	C	0.65303	0.37045	0.30511
O20	O	0.95317	0.78608	0.37555
N21	N	0.89590	0.80984	0.44090
N22	N	0.93298	0.85985	0.49977
C23	C	0.92165	0.89448	0.55506
C24	C	0.96090	0.94651	0.65751
C25	C	0.90891	0.77389	0.38987
C26	C	1.03279	0.64824	0.68063
C27	C	1.07488	0.65150	0.89332
N28	N	1.12604	0.67216	0.75051
C29	C	1.16800	0.68166	0.95956
H30	H	0.90954	0.97553	0.65324
H31	H	0.75634	0.63712	0.06345
H32	H	0.88730	0.58049	1.02625
H33	H	0.90384	0.64468	1.02211
H34	H	0.95081	0.65564	0.51970
H35	H	0.92951	0.58938	0.51721
H36	H	0.97492	0.59647	0.99651
H37	H	0.99218	0.66150	1.04029
H38	H	0.84505	0.76682	-0.03076
H39	H	0.80892	0.53397	0.29131
H40	H	0.78295	0.44690	0.29047

H41	H	0.64232	0.39905	0.30462
H42	H	0.85804	0.79944	0.45855
H43	H	0.88260	0.88476	0.55940
H44	H	1.04308	0.68506	0.57705
H45	H	1.02459	0.62031	0.49538
H46	H	1.05958	0.61201	0.96844
H47	H	1.07637	0.67415	1.09031
C48	C	1.14134	0.72281	0.62057
C49	C	1.12340	0.63207	0.54981
H50	H	0.29843	0.50329	0.83786
H51	H	0.35332	0.52053	1.02853
H52	H	0.29332	0.46569	1.14597
H53	H	0.40445	0.51134	0.67461
H54	H	0.36181	0.52279	0.48777
H55	H	0.37583	0.47457	0.35948
H56	H	0.27742	0.39783	0.41733
H57	H	0.25459	0.43652	0.56285
H58	H	0.25413	0.38951	0.79544
H59	H	0.94249	0.98450	0.29751
H60	H	0.91263	0.69998	0.66966
H61	H	0.96023	0.94568	0.91273

References

- [1] L. Ma, N. A. Qaisrani, M. Hussain, L. Li, Y. Jia, S. Ma, R. Zhou, L. Bai, G. He, F. Zhang, Cyclodextrin modified, multication cross-linked high performance anion exchange membranes for fuel cell application, *J. Membr. Sci.* 607 (2020) 118190.
- [2] Q. Yang, C. X. Lin, F. H. Liu, L. Li, Q. G. Zhang, A. M. Zhu, Q. L. Liu, Poly (2,6-dimethyl-1,4-phenylene oxide)/ionic liquid functionalized graphene oxide anion exchange membranes for fuel cells, *J. Membr. Sci.* 552 (2018) 367-376.
- [3] R. Devanathan, A. Venkatnathan, M. Dupuis, Atomistic Simulation of Nafion Membrane: I. Effect of Hydration on Membrane Nanostructure, *J. Phys. Chem. B* 111 (2007) 8069-8079.
- [4] S. G. Lee, T. A. Pascal, W. Koh, G. F. Brunello, W. A. Goddard, S. S. Jang, Deswelling Mechanisms of Surface-Grafted Poly(NIPAAm) Brush: Molecular Dynamics Simulation Approach, *J. Phys. Chem. C* 116 (2012) 15974-15985.
- [5] W. H. Kyung, H. K. Kwan, A. H. Khaldoun, B. Chulsung, J. S. Young, S. J. Seung, Molecular Dynamics Simulation Study of a Polysulfone-Based Anion Exchange Membrane in Comparison with the Proton Exchange Membrane, *J. Phys. Chem. C* 118 (2014) 12577-12587.
- [6] B.V. Merinov, W.A. Goddard III, Computational modeling of structure and OH⁻ anion diffusion in quaternary ammonium polysulfone hydroxide-polymer electrolyte for application in electrochemical devices, *J. Membr. Sci.* 431 (2013) 79-8.
- [7] W. Zhang, A. C. T. van Duin, ReaxFF Reactive Molecular Dynamics Simulation of Functionalized Poly(phenylene oxide) Anion Exchange Membrane, *J. Phys. Chem. C* 119 (2015) 27727-27736.

- [8] V. Dubey, A. Maiti, S. Daschakraborty. Predicting the solvation structure and vehicular diffusion of hydroxide ion in an anion exchange membrane using nonreactive molecular dynamics simulation, *Chem. Phys. Letters* 755 (2020) 137802.
- [9] J. L. D. Salvo, G. D. Luca, A. Cipollina, G. Micale, Effect of ion exchange capacity and water uptake on hydroxide transport in PSU-TMA membranes: A DFT and molecular dynamics study, *J. Membr. Sci.* 599 (2020) 117837.
- [10] Z. Li, X. Y. He, Z. Jiang, Enhancing hydroxide conductivity and stability of anion exchange membrane by blending quaternary ammonium functionalized polymers, *Electrochimica Acta*, 240 (2017) 486.
- [11] W. Sheng, X. Zhou, L. Wu, Quaternized poly(2,6-dimethyl-1,4-phenylene oxide) anion exchange membranes with pendant sterically-protected imidazoliums for alkaline fuel cells, *J. Membr. Sci.* 601 (2020) 117881.
- [12] H. Zhu, R. Li, F. H. Wang, Poly tris(1-imidazolyl) benzene ionic liquids/poly (2, 6-dimethyl phenylene oxide) composite membranes for anion exchange membrane fuel cells, *J. Membr. Sci.* 52 (2017) 11109.
- [13] P. F. Msomia, P. T. Nonjola, P. G. Ndungu, Poly (2, 6-dimethyl-1, 4-phenylene)/polysulfone anion exchange membrane blended with TiO₂ with improved water uptake for alkaline fuel cell application, *Int. J. Hydrog. Energy* 45 (2020) 29465.
- [14] M. Kumari, J. C. Douglin, D. R. Dekel, Crosslinked quaternary phosphonium-functionalized poly(ether ether ketone) polymer-based anion-exchange membranes, *J. Membr. Sci.* 626 (2021) 119167.

[15] X. Chu, J. Liu, S. Miao, Crucial role of side-chain functionality in anion exchange membranes: properties and alkaline fuel cell performance, *J. Membr. Sci.* 625 (2021) 119172.